

Diffraction & Interference

Duncan Beauch with Charlotte Hoelzl

October 19, 2021

I. Introduction

Waves encountering barriers or other waves produce complicated and spectacular interactions. One of these is diffraction, when a wave encounters an opening such as a slit in a barrier. The resulting wave on the other side appears to propagate in all directions with the other end of the opening acting as the origin of the wave. Another property of waves is superposition, which occurs when a wave encounters another wave. The result where these waves mix is a new wave which is the sum of the two waves. These two properties can be observed at the same time in one of the most famous experiments in modern physics: the double slit experiment, in which the two phenomena can be observed in light due to its wave-like properties. The resulting interference pattern can be used to determine the conditions of the setup such as the distance between slits, distance from the slits, and diffraction angle. In the following experiments we will use various slit-laser setups to verify the known equations about the diffraction of light by studying their interference patterns, specifically the minima and maxima of the intensity of light to determine the slit width b .

II. Single Slit Diffraction

Here we will study the diffraction of light through just a single slit. The setup for each of the following experiments will be nearly identical and a diagram is shown below in Figure 1.

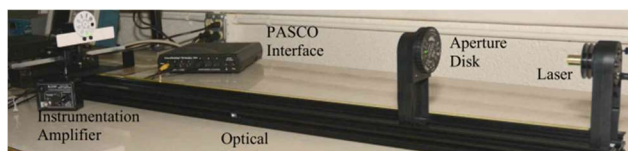


Figure 1: Laser/aperture setup

On one end of the track is the PASCO laser which produces a green beam with wavelength $\lambda = 532.4$ nm and will be used for all experiments. The aperture disk is inserted as close to the laser as possible and can be rotated to change the opening to various sizes and exchanged for disks with multiple slits for later experiments. At the other end of the track is a high sensitivity light sensor whose gain can be adjusted to record various intensities of light. This is connected to Capstone via the PASCO interface and plots are made in real time which will be used to study the resulting diffraction patterns. To increase the precision of our measurements, each experiment will be carried out in as dark as environment as possible. Ambient light from computer screens will play a role in adding uncertainty to our data requisition which will be seen in the resulting plots.

Using the single slit aperture disk, we can observe patterns resulting from diffraction through slits of sizes 20, 40, 80, and 160 microns. The diffraction patterns for all sizes appears as a dotted horizontal line on the viewing screen where the maxima are located at the center of each dash with the central dash being the largest and most intense and these effects diminish the further from the center. As the slit size increases, the number of dashes increase and spacing between each dash decrease. The diffraction patterns for 20 and 160-micron slits can be seen in Figures 2 and 3 respectively.



Figure 2: Diffraction pattern for a single slit of 20 microns.

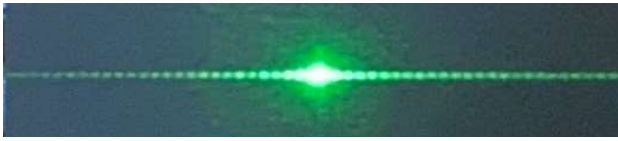


Figure 3: Diffraction pattern for a single slit of 160 microns.

After viewing the full patterns created by the slits, we now want to record the intensity as a function of position. In order to do this, the light sensor is able to move perpendicular to the laser and capture the intensity of light at each position along the diffraction pattern. The diffraction pattern for all four slit widths are shown in Figures 4, 5, 6, and 7. Using our measured distance D , known wavelength λ , and x-coordinates of the first minima we can use the following formula to estimate the slit width b_{exp} that created the resulting pattern:

$$b_{exp} = \frac{2D\lambda}{\Delta x}$$

The calculated slit widths along with relevant measurements are shown in Table 1. Many of the calculated values for b are off by a significant amount which was most likely caused by improper measurement of the distance D . Another source of error is the ambient light that was present in the room. As you can see in the intensity graphs, where the minima occur the intensity value should be zero, but some light is being detected, nonetheless. Additionally, the equation to estimate b above is a small angle approximation for $\sin(\theta_1)$.

Notice as the slit size increases, the shape of the intensity graph varies drastically. The central maximum has a much stronger intensity and subsequent lesser maxima to the sides decrease in amplitude and width.

Table 1: Estimating b		
b (μm)	b_{exp} (μm)	Δx (mm)
20	16.2	65.3
40	37.1	28.6
80	75.0	14.1
160	158.1	6.7

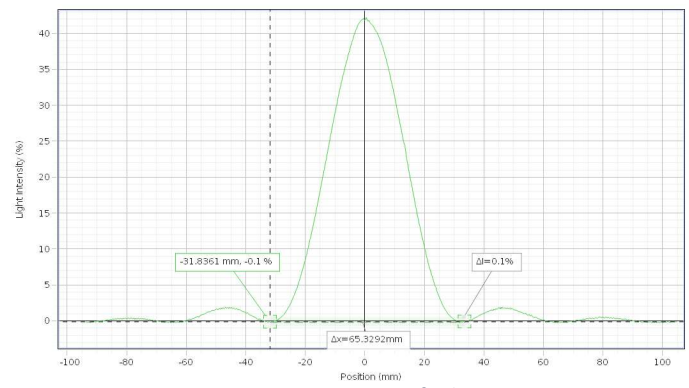


Figure 4: Intensity vs. position for $b=20$ microns

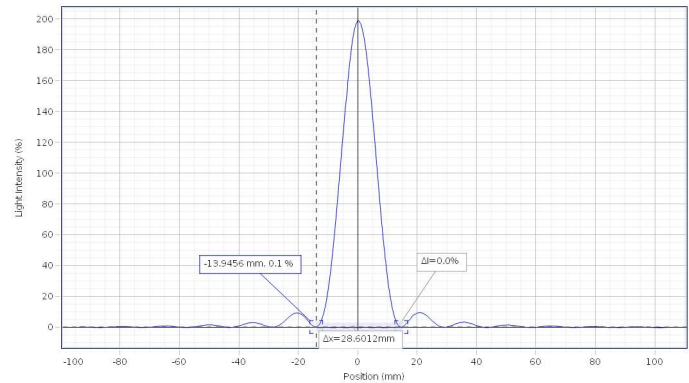


Figure 5: Intensity vs. position for $b=40$ microns

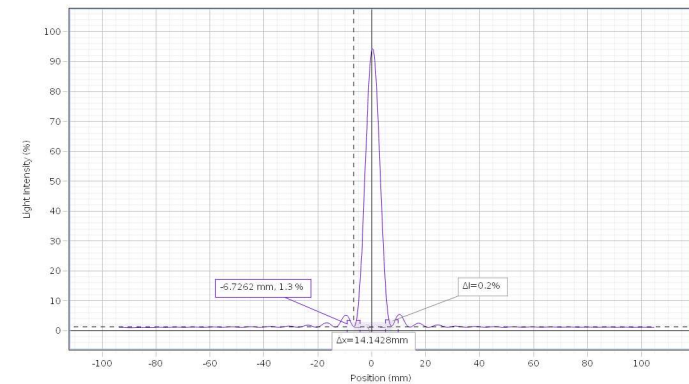


Figure 6: Intensity vs. position for $b=80$ microns

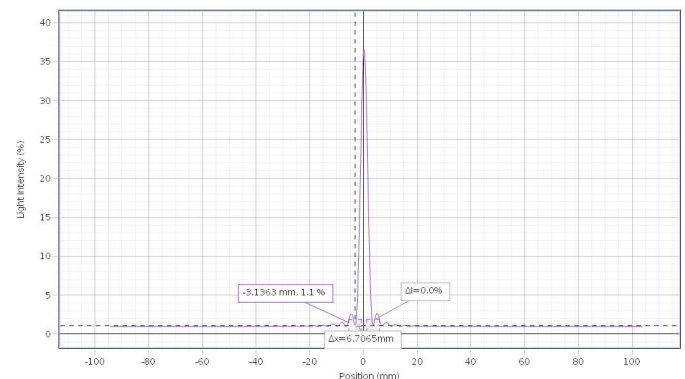


Figure 7: Intensity vs. position for $b=160$ microns

Now rather than having an estimate for the value of b we can use a more robust yet tedious method. We return to the 40-micron slit and record the intensity vs. position graph, labeling every maximum up to $n=6$ peaks away from the central maximum in both the position and negative directions. This results in twelve maxima and six Δx values which represent the distance between two maxima of the same order n . These will allow us to calculate b using the following equations:

$$\sin(\theta_n) = \frac{1}{\sqrt{1 + \frac{2D}{\Delta x^2}}}$$

$$\sin(\theta_n) = \frac{n\lambda}{b}$$

Plotting $\sin(\theta_n)$ vs. n should yield a straight line with a slope of $\frac{\lambda}{b}$. Since we know $\lambda=532.4$ nm we can calculate the value of b by multiplying the slope of our plot by λ . The relevant data is shown in Table 2, plot of $\sin(\theta_n)$ vs. n in Figure 8, and least squares regression fit in Table 3.

The estimated slit width obtained through this method was $b_{exp} = 36.58 \mu\text{m}$, a value that differs from the known value for $b = 40 \mu\text{m}$ by 8.6%. This error could have occurred for the same reasons as stated before: ambient light interfering with the light sensor or a miscalculated distance D .

Table 2: $\sin(\theta_n)$ vs. n		
N	Δx (mm)	$\sin(\theta_n)$
1	28.96	0.0145
2	58.33	0.0293
3	87.07	0.0437
4	116.77	0.0585
5	144.92	0.0726
6	174.90	0.0875

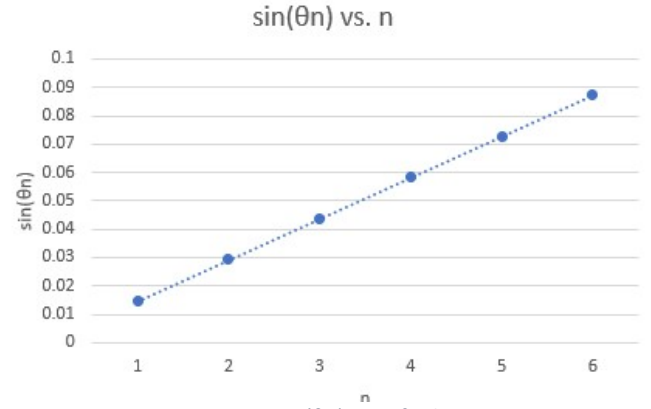


Figure 8: $\sin(\theta_n)$ vs. n for $b=40\mu\text{m}$

Table 3: $\sin(\theta_n)$ vs. n Slope	
Slope	
Value	0.01455
Error	0.000048
Correlation	0.99996

III. Multiple Slit Interference

Now that we are comfortable with the diffraction property of light, we can introduce superposition. To do this, we use a new aperture in front of the laser which can be set to have multiple slits. Again, we want to determine a way to calculate the width b of the slit that created the interference pattern shown. This can be done by manipulating a series of equations shown below:

$$I/I_{\max} = \cos^2(\gamma) \text{sinc}^2(\beta)$$

$$\gamma \equiv \pi d \sin(\theta) / \lambda$$

$$\beta(\theta) \equiv \frac{\pi b \sin(\theta)}{\lambda}$$

$$d = \frac{m\lambda}{\sin(\theta_m)}$$

$$\sin(\theta_n) = \frac{1}{\sqrt{1 + \frac{2D}{\Delta x_m^2}}}$$

Thus, we can solve for b_{exp} by finding the distance between principal maxima of the same order m , distance from the laser to the sensor D , and our known wavelength λ . These values were found using the setup described earlier for apertures with number of slits $N = 2, 3, 4$, and 5 . The relevant data can be seen in Table 4 and intensity vs. position plots are shown in Figures 9, 10, 11, and 12 respectively.

Table 4: Multiple Slits		
N	Δx (mm)	b (μm)
2	29.88	36.58
3	29.67	36.92
4	29.15	37.22
5	29.05	37.36

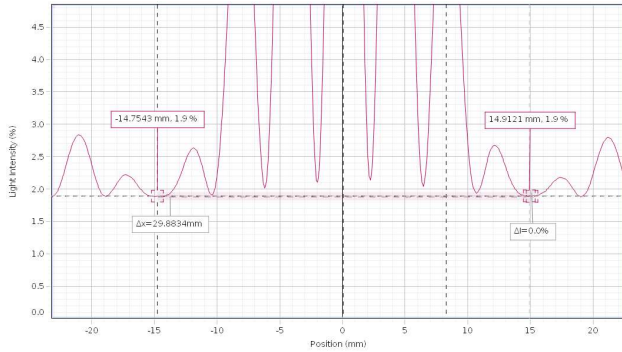


Figure 9: Intensity vs. position for $N=2$

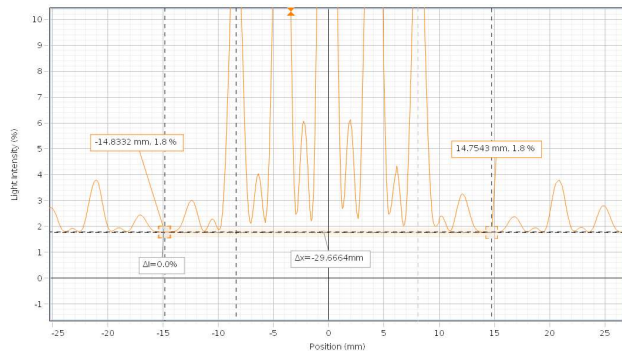


Figure 10: Intensity vs. position for $N=3$

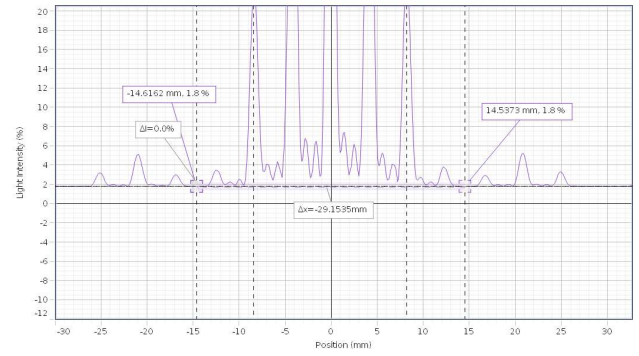


Figure 11: Intensity vs. position for $N=4$

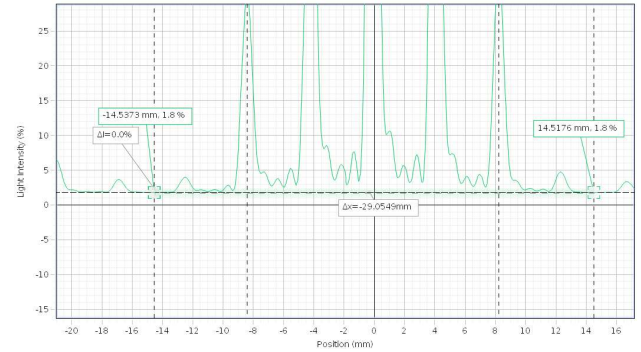


Figure 12: Intensity vs. position for $N=5$

Similar to our first experiment we can take one of our diffraction patterns and by analyzing the positions of certain maxima, we can obtain a least squares regression that will tell us about an important value. In this case, we will find the differences in the locations of the principal maxima for the $N=5$ case. Using the same small angle approximation, we can find $\sin(\theta_m)$ which relates to the slit spacing d as follows:

$$\sin(\theta_m) = \frac{m\lambda}{d}$$

Plotting $\sin(\theta_m)$ vs. m will result in a straight line with slope $\frac{\lambda}{d}$ and with our known $\lambda = 532.4 \text{ nm}$, we can determine d . The relevant values are shown in Table 5, plot of $\sin(\theta_m)$ vs. m in Figure 13, and least-squares regression fit in Table 6. Notice for $m = 7$, there is a suppressed maxima due to the envelope pattern of sinc^2 . The value obtained by the plot of $\sin(\theta_m)$ vs. m is $d_{exp} = 126.5 \mu\text{m}$ which differs from the expected value of $d = 125 \mu\text{m}$ by only 1.2%.

Table 5: $\sin(\theta_m)$ vs. m for $N=5$		
m	Δx (mm)	$\sin(\theta_m)$
1	8.28	0.0042
2	16.6	0.0083
3	24.8	0.012
4	33.6	0.017
5	41.8	0.021
6	50.1	0.025
7	N/A	N/A
8	67.1	0.033
9	75.4	0.038

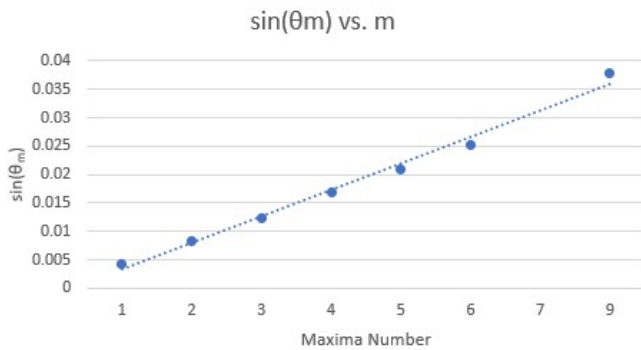


Figure 13: $\sin(\theta_m)$ vs. m for $N=5$

Table 6: $\sin(\theta_m)$ vs. m	
Slope	
Value	0.00421
Error	0.0000088
Correlation	0.999974

IV. Diffraction by circular Apertures and Discs

We are now returning to the single slits aperture disk except this time we will have openings as either holes or opaque dots. The setup remains the same with slightly a slightly different value for $D = 96$ cm. This diffraction pattern is much different than the previous single slit as it consists of concentric circles with increasing diameter. We can determine the diameter of the aperture hole d using the following equations:

$$\tan(\theta) = \frac{w}{2D}$$

$$\sin(\theta) = 1.22 \frac{\lambda}{d}$$

Where w represents the diameter of the diffraction pattern. Using the measured diameter $w = 1.9$ cm, we can solve for $d = 65.64 \mu\text{m}$.

Now we will change the aperture to dots. The dots aperture has the same diameter as the holes in a random arrangement except they are opaque instead of holes. Babinet's Principle tells us that the diffraction pattern here should be the same except for the bright central maximum that occurs for holes. The process for holes was repeated for the dots setting and using the same set of equations we measure the diameter of the diffraction pattern to be $w = 1.87$ cm and $d = 66.69 \mu\text{m}$. These values of d differ by only 1.6%, confirming Babinet's Principle.

We can use this method of diffraction to study the size of microscopic objects to a great deal of precision. To show this we will perform the same experiment with a glass slide covered in lycopodium powder, a pollen consisting of spherical particles. Replacing the aperture disk with the pollen-covered slide we get a very similar diffraction pattern and using the same system of equations we find that the diameter d of the pollen particles to be $40.23 \mu\text{m}$. The average lycopodium particle is about $33 \mu\text{m}$, very close to our experimental value. This should not be taken as a judgement of the accuracy of the procedure however, because pollen size can vary from case to case.

Similarly, another microscopic object we can study with this method is the width of a human hair. Using the hair of Charlotte, with consent, the width of the hair was measured to be $d = 67.4 \mu\text{m}$, a measurement that falls within the expected region for hair width. This again proves the usefulness and accuracy of Babinet's Principle.

V. Diffraction Grating

Diffraction gratings are in essence a number of organized slits N called the grating constant which are compressed to a very fine space.

Their spacing d can then be represented as $\frac{1}{N}$.

The pattern produced by such an aperture is unlike that of smaller N slits. Rather than concentrating the intensity within a relatively small angle with many maxima, diffraction gratings spread very intense maxima at large angles θ_m given by the following equation:

$$\sin(\theta_m) = \frac{m\lambda}{d}$$

Now we seek to measure the grating constant N . To do this we will find the angles θ_m that produce maxima. The diffraction grating is placed in front of the laser and its diffraction pattern scatters in all directions. To measure the angle, the grating is placed at the center of a rotational plate marked with angles from the center. A paper is then marked with the central maxima and rotated around the disk until the first three order maxima are found and their angle recorded. The data can be seen in Table 7. The grating constant N is calculated by rearranging the above equations:

$$N = \frac{\sin(\theta_m)}{m\lambda}$$

The average N over all six calculated N is 580.7, which differs from the expected value of 600 by 3.2%.

VI. Conclusion

Throughout these four experiments we have shown several important properties of diffraction patterns. First, given the diffraction pattern of light with specified wavelength, we can use our equations to solve for the width of the opening the light passed through. Additionally, we proved Babinet's Principle in Experiment 3 which tells us that we can also tell the width of an object based on its diffraction pattern with specified wavelength. From experience working with diffraction patterns, we can tell the shape of the obstacle the light passed through because each shape has a distinct pattern. These principles together allow us to do many precise microscopic measurements that would otherwise be impossible for our macroscopic selves. We know that light is not the only way diffraction patterns can be created. Other particle beams such as electrons can be used to study objects even smaller than for light because their wavelength can be even shorter. This is important especially for nuclear physics in which objects being measured are less than the scale of an atom, something that light could not be used to probe. Understanding the relationship between diffraction patterns and their causal conditions is important for the future of physics research.

Table 7: Calculated Grating Constants

m	Angle (°)	Grating Constant N
-3	-69	585
-2	-38	578
-1	-18	580
1	18	580
2	38	578
3	68.5	583